SCIENCE CHINA
Chemistry

•REVIEWS•
SPECIAL ISSUE: Celebrating the 100th Anniversary of Chemical Sciences in Nanjing University

May 2020 Vol.63 No.5: 648–664
https://doi.org/10.1007/s11426-019-9699-3

Responsive boron biomaterials and their biomedical applications

Weizhi Chen[†], Xu Zhen[†], Wei Wu & Xiqun Jiang[*]

MOE Key Laboratory of High Performance Polymer Materials and Technology, Department of Polymer Science & Engineering, College of Chemistry & Chemical Engineering, and Jiangsu Key Laboratory for Nanotechnology, Nanjing University, Nanjing 210093, China

Received December 31, 2019; accepted February 10, 2020; published online April 21, 2020

Due to the formation of dynamic boronate ester bonds between phenylboronic acid (PBA) and 1,2- and 1,3-diols, PBA-containing biomaterials show increasing applications in biomedical areas, including responsive nanobiomaterials for targeting delivery of chemical drugs, protein drugs, gene drugs and imaging agents *in vitro* and *in vivo* for detection of various bioactive molecules such as sialic acid, saccharides, adenosine triphosphate (ATP) and dopamine. With the specific reaction between PBA and sialic acid, which is overexpressed in many kinds of cancer cells, PBA has been used as a targeting moiety for tumor-targeting drug delivery. Additionally, PBA as an electron acceptor affords nanomaterials Lewis acid-base coordination with electron donor atoms such as nitrogen and oxygen, which can be exploited for developing drug delivery systems with high drug loading. Furthermore, PBA-containing materials can stoichiometric consume reactive oxygen species (ROS) and show a nucleus targeting ability. This current review outlined PBA-containing biomaterials with various responsive abilities including sialic acid-targeting, sugars-binding, ROS-response, ATP-response, dopamine-binding, and nuclear targeting. On this basis, their biomedical applications were summarized.

responsive biomaterials, phenylboronic acid, drug delivery system, biomedical application

Citation: Chen W, Zhen X, Wu W, Jiang X. Responsive boron biomaterials and their biomedical applications. *Sci China Chem*, 2020, 63: 648–664, https://doi.org/10.1007/s11426-019-9699-3

1 Introduction

Organoboron (aryl boronic acid especially for PBA) is an important group in organic reaction and shows significant potentials in biological fields [1,2]. PBAs are initially used for the separation of saccharides and related compounds through a chromatographic method [3]. With the development of material science and biomedical technology, more and more molecules with bioactivity are found to interact with PBAs including sialic acid overexpressed on the surface of cancer cells [4], ROS overproduced in inflammation and tumorigenesis [5], ATP, which is a general energy source for life activities [6], and dopamine, which is an important neurotransmitter and involved in cellular communications and signals transductions [7]. Thus, all of them can be used as targets for disease therapy and diagnosis through PBA-containing biomaterials since PBA groups can form dynamic boronate ester bonds with diol molecules including sialic acid, saccharides, ATP, dopamine, and can interact with electron donor groups such as amines, and also can stoichiometrically consume ROS [8–11].

In this review, we will summarize the recent advances in the development of responsive boron biomaterials for biomedical applications including: 1) PBA-containing biomaterials targeting sialic acid for tumor-targeting drug delivery and detection; 2) saccharides-binding PBA-containing biomaterials exploited for glucose-responsive insulin release, capture and release of various cells, and self-healing materials; 3) N-B coordination of PBA-containing drug delivery systems with high drug loading; 4) ROS-responsive PBA-containing nanocarriers for drug delivery and ROS sensors;

†These authors contributed equally to this work.
*Corresponding author (email: jiangx@nju.edu.cn)

5) ATP-responsive PBA-containing drug carriers and ATP detectors with ATP-responsive property; 6) dopamine-responsive PBA-containing detection systems; 7) nuclear targeting PBA-containing nano biomaterials for nuclear-targeting drug delivery (Figure 1). Finally, we analyze the potential challenges and perspectives of PBA-containing nanobiomaterials in the biomedical area.

2 Responsive boron biomaterials and their applications in biomedical areas

2.1 Structures of PBA in PBA-containing biomaterials

In aqueous media, there is an equilibrium between trigonal form (SP^2) and the tetrahedral form (SP^3) of PBAs (Figure 2). PBAs in the trigonal form are nonionic and hydrophobic, which can become hydrophilic after interaction with a hydroxide ion in an alkaline solution [12]. The pH-induced hydrophilic-hydrophobic transformation can be utilized to control the assembly and disassembly of boron copolymers into micelles as well as drug release. The complexation between PBA and polyol compounds is also an equilibrium and is affected by pH [13]. Stable boronate ester bonds are formed in solutions with pH higher than the pK_a of PBA and will dissociate as pH reduced. This reversible reaction allows PBA containing materials to act as pH-sensitive or diol-sensitive materials to react with biomolecules such as sialic acid [14], saccharides [15], ATP [16] and dopamine. These properties are the foundation for exploiting PBA-containing materials with targeting abilities and stimulus-responsiveness.

However, pK_a of PBA is about 8.8 and the optimal pH associated with sugars is generally above 9.0, which is not suitable for applications in a physiological environment. There is a wealth of research exploiting to modify PBA into materials responsive to the physiological pH range. The pK_a values of PBAs can be adjusted from 4.2 to 9.0 through the introduction of electron-withdrawing groups including fluoro and nitro or electron-donating groups [17]. Comparing to PBA, 5-amino-2-hydroxymethylphenylboronic acid (benzoxaborole) has a higher affinity for saccharides [18].

The affinity constants of PBA for D-fructose, D-glucose, and Neu5Ac are 128, 5 and 13 M^{-1}, respectively [18]. However, the affinity constants of benzoxaborole for D-fructose, D-glucose, and Neu5Ac are much higher, which are 336, 28 and 43 M^{-1}, respectively [18]. It should be noted that PBAs with different substituents have different binding affinities with diols and the optimal binding pH is not always above the pK_a of PBAs especially for a multicomponent complex system.

2.2 Sialic acid-binding PBA-containing biomaterials

Sialic acid, also known as *N*-acetylneuraminic acid (Neu5Ac), usually links with the outside of glycan chains [19]. The sialylation modification is very vital for many bioprocesses including cellular signaling, adhesion, and recognition [20,21]. Sialic acid, which is overexpressed in various cancers such as breast, lung, and colon cancers [22], is highly related to cancer progression, metastases, and poor prognosis [4]. Therefore, sialic acid is an ideal target for cancer therapy.

The conformation of the complex between 3-(propionamido) phenylboronic acid (PAPBA) and sialic acid is shown in Figure 3. Sialic acid binds PAPBA through the glycerol side chain and there is an equilibrium between the two type complexes. Otsuka *et al.* [23] found that the equilibrium constant (K) of PAPBA complexation with Neu5Ac (37.6 M^{-1}) at pH 7.4 was significantly higher than that of PAPBA complexation with glucose (5.1 M^{-1}). When the pH in-

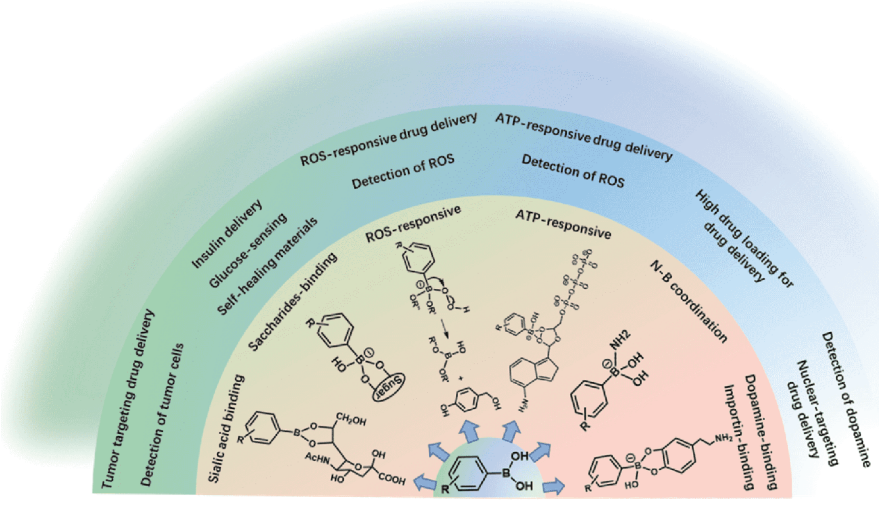

Figure 1 The responsive boron biomaterials mentioned in this review and their applications in biomedical areas (color online).

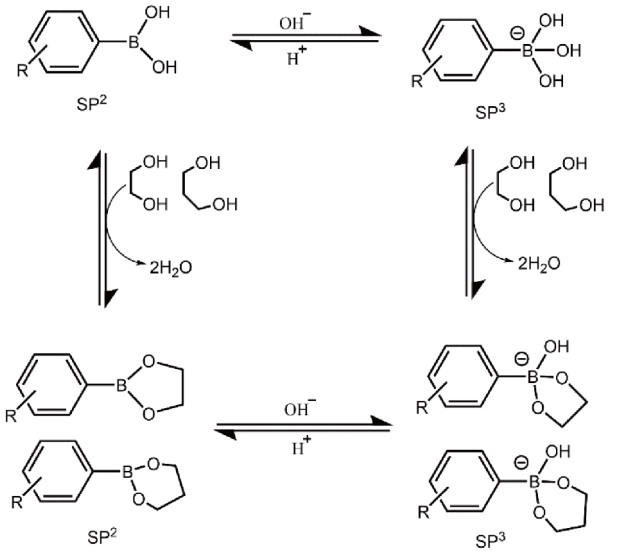

Figure 2 The equilibrium interaction between PBA and diols in aqueous solution influenced by pH alteration.

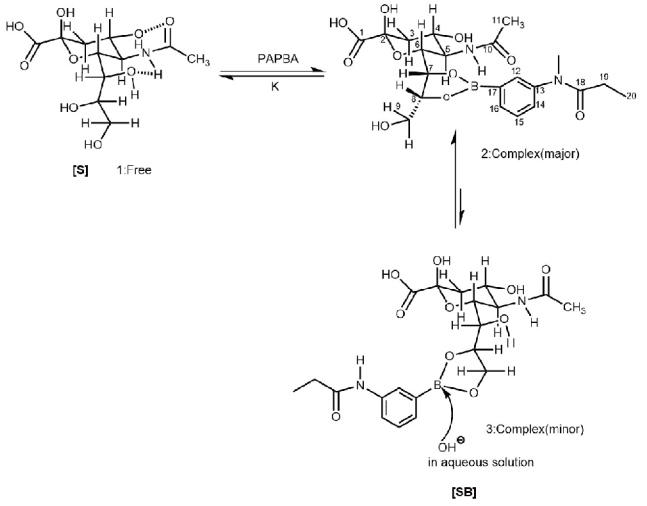

Figure 3 The interaction between PAPBA and sialic acid, adapted with permission from Ref. [23], copyright by American Chemical Society (2003).

creased from 4 to 10, the equilibrium constant for the complexation between PAPBA and sialic acid decreased gradually from 40 to 20 M^{-1}. For the complexation between PAPBA and glucose, the equilibrium constant increased gently (from 0 to 5.1 M^{-1}) before pH 7.4 and dramatically (from 5.1 to 70 M^{-1}) after pH 7.4. The larger retention time for sialic acid on boronate affinity chromatography at pH 6.5 further verified the high complexing ability of sialic acid with APBA. The high selectivity of APBA for sialic acid in low pH is suitable for tumor targeting due to the weak acid tumor microenvironment (pH=6.5).

2.2.1 Tumor targeting drug delivery

Taking advantage of the high association constant between PBA and sialic acid at the weak acidic environment, PBA-containing materials have been widely utilized for tumor targeting therapy [24–26]. Due to the development of a simple and environmental-friend method for preparing PBA-incorporated nanoparticles without using any organic solvent, PBA-containing biomaterials were firstly applied for tumor-targeting drug delivery *in vivo* [27,28]. The polymerization of APBA was processed in the presence of bovine serum albumin (BSA) or chitosan (CS), and then poly-APBA (PAPBA)-riched nanoparticles were produced spontaneously in water. PBA-contained BSA nanoparticles with different diameters were synthesized by simply adjusting the solution pH. The PBA-rich BSA nanoparticles could retent in the tumor site as long as 13 days, which was much longer than 8 days for BSA nanoparticles, through the interaction between PBA groups and the overexpressed sialic acid in tumors. PBA-based CS nanoparticles were further synthesized, following modification with iRGD to obtain a dual tumor-targeting ability and an enhanced tumor penetration ability verified both in multicellular spheroids and subcutaneous H22 tumor. After the encapsulation of DOX, PBA-decorated CS nanoparticles showed a higher tumor accumulation and preferable anticancer efficacy for subcutaneous H22 tumors than non-decorated CS nanoparticles, due to the PBA mediate tumor-targeting ability [29].

Further, elastin-like polypeptide (ELP) with lysine residues was expressed from *Escherichia coli* and PBA-incorporation ELP nanoparticles were prepared through the coordination between PBA and the amino in ELP [30]. As shown in Figure 4, PAPBA-ELP nanoparticles showed efficient cellular uptake in SH-SY5Y cells and tumor-targeting ability in H22 tumor-bearing mice. When the cancer cells were pre-administrated with free PBA or sialic acid, the cellular internalization of PAPBA-ELP nanoparticles was significantly decreased, indicating that the PAPBA-ELP nanoparticles entered into tumor cells via the binding of PBA and the overexpressed sialic acid on the surface of tumor cells. The nanoformulation could improve tumor accumulation and decrease cardiotoxicity, comparing to free doxorubicin (DOX). The tumor growth inhibition rates of drug-loaded nanoparticles and free drug in an H22 tumor model, are 81% and 48%, respectively, indicating that PAPBA nanoparticles exhibited a superior anticancer efficacy comparing to free DOX. Zhang *et al*. [31] synthesized a variety of giant multi-arm block copolymers with different hydrophilic blocks including polyethylene glycol (PEG) and poly(carboxybetaine) with or without PBA-functionalization. PBA-introduced multi-arm copolymer showed improved capacities in cellular internalization, tumor accumulation, and penetration.

The penetration behaviors of drugs and nanocarriers in solid tumors are a great challenge and is vital for the effective delivery of drugs into tumors. Degradation of the condense

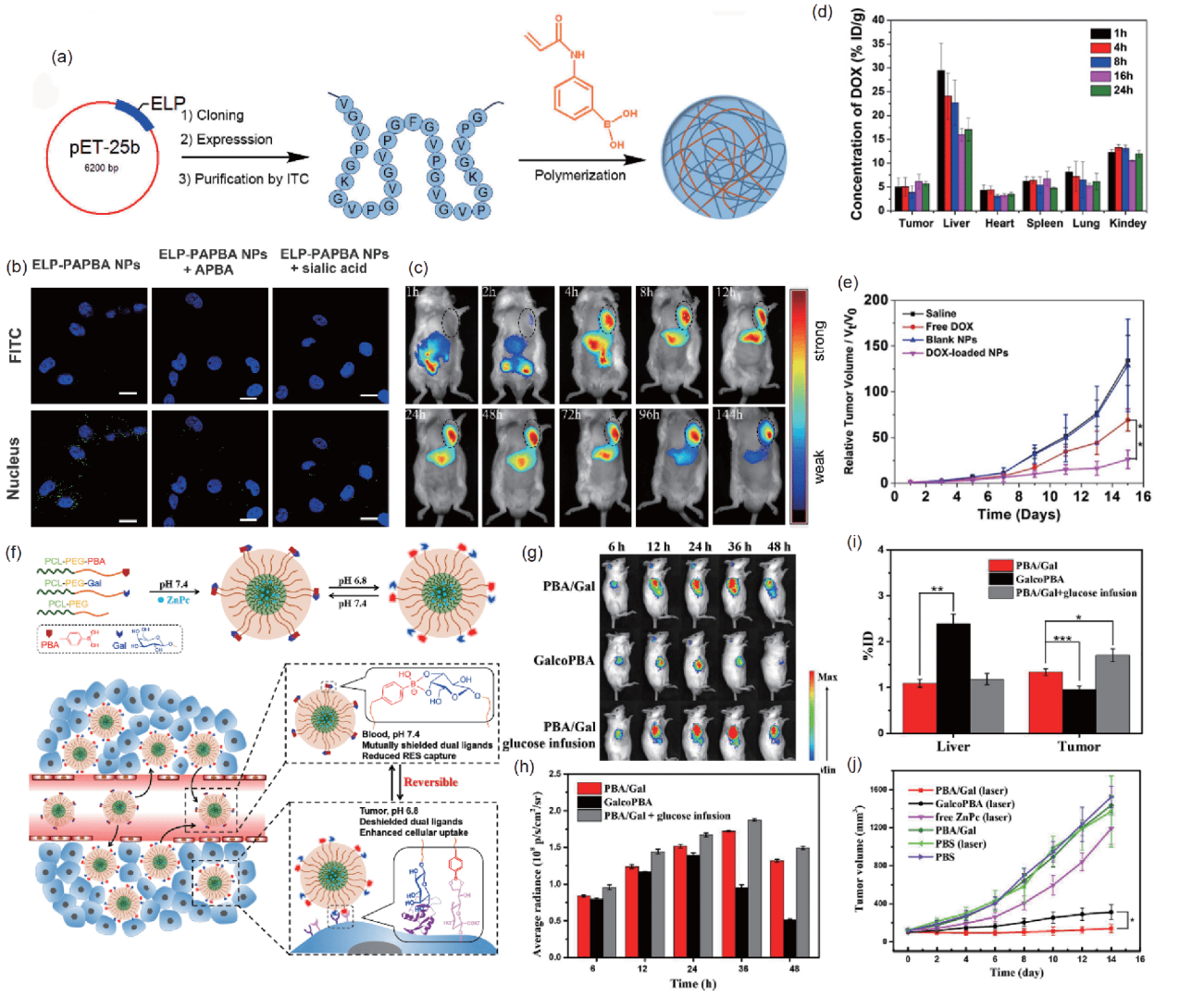

Figure 4 PBA-containing materials-based drug delivery systems used for sialic acid-targeting tumor therapy. (a) Illustration of the synthesis of PBA-rich ELP nanoparticles. (b) CLSM images of PBA-rich ELP nanoparticles incubated in SY5Y cells with or without pretreatment of free PBA and sialic acid. (c) Real-time NIR imaging of PBA-rich ELP nanoparticles in H22 tumor-bearing mice. The biodistribution (d) and anticancer effect (e) of DOX-loaded PBA-rich ELP nanoparticles in mice bearing H22 tumors, adapted with permission from Ref. [30], copyright by the Royal Society of Chemistry (2017). (f) Schematic diagram of the synthesis and tumor targeting of PBA/Gal dual-target micelles. (g) NIR images of tumor-bearing mice at different times after intravenous injection with a different formulation. (h) Quantitative analysis of the fluorescence intensity change of different micelles in tumor sites at different times. (i) Measurement of ZnPc content in tumors and livers of mice with different treatments. (j) Antitumor efficacy of different formulations, adapted with permission from Ref. [36], copyright by American Chemical Society (2019) (color online).

extracellular matrix and alleviation of the large tumor interstitial fluid pressure (IFP) and tumor stress are optional strategies. More recently, Qian *et al*. [32] prepared PBA-decorated soy protein (SPB) nanoparticles with various diameters through the interaction between PBA and soy protein (SP). It is noted that when SPB nanoparticles with a size of 30 nm were intravenously injected into mice bearing H22 tumor, the tumor IFP decreased gradually with the dosage of nanoparticles increased from 50 mg/kg, and reached plateau when the dosage increased to 150 mg/kg demonstrating that 150 mg/kg was the optimal dosage. This dosage was further used for evaluating the capacity of SPB nanoparticles to reduce the solid stress of CT26 tumors. Comparing to SPB nanoparticles with 50 and 150 nm, SPB nanoparticles with 30 nm lowered the tumor stress by about 50%. The ability of SPB nanoparticles to reduce tumor IFP and solid stress offers the opportunity to deliver more drugs to tumors. Collaborating with the sialic acid-targeting ability of PBA groups, DOX-loaded SPB nanoparticles (with a drug loading content as high as 27%) showed a favorable tumor accumulation, resulting in a great anticancer effect in H22 tumor-bearing mice.

Recently, Pan's group [33] reported PBA modified PEGylated polydopamine (PDA) nanoparticles through the dynamic interaction between PBA and diols. Owing to the acid-cleavable feature of the borate ester bonds, the nano-

particles could be dePEGylated once reaching the weakly acidic tumor environment, leading to the exposure of PBA groups for tumor targeting. Moreover, the PDA core and the loaded chemical drug provide a combination of photothermal therapy and chemotherapy. With the nitrogen-boron (N-B) coordination between PBA groups and amine groups in drugs, the incorporation of PBA moiety into polymers can promote drug loading, resulting in pH-induced drug release [34]. His group introduced fructose to block the PBA-affinity chemistry in normal tissues, thus reducing the drug accumulation and side effects in normal tissues [35]. The fructose moiety departed in the weak acid tumor environment, allowing exposure of PBA groups in nanoparticles to interact with the overexpressed sialic acid on cancer cells thus enhancing the accumulation of the nanoparticles in tumor sites. To improve tumor targeting ability, a dual-targeting strategy can be applied. For example, Yuan and co-worker [36] have prepared sialic acid and asialoglycoprotein receptor (ASGPR) dual-target micelles through the assembly of PBA-conjugated poly(ethylene glycol)-*b*-poly(ε-caprolactone) (PBA-PEG-PCL) and galactose-conjugated poly(ethylene glycol)-*b*-poly(ε-caprolactone) (Gal-PEG-PCL). In the neutral physiological environment, PBA groups are binding with Gal groups through boronate ester bonds. When the micelles reached weak acid tumor microenvironment with a pH of about 6.8, the boronate ester bonds could be broken, allowing the exposure of the PBA groups and Gal groups to bind sialic acid and ASGPR, respectively, achieving a dual-targeting function (Figure 4(f)). The dual-target micelles can be applied as nanocarriers for photosensitizer zinc phthalocyanine (ZnPc) encapsulation and photodynamic therapy (PDT). After reduced the tumor extracellular pH by glucose infusion, the tumor accumulation of ZnPC-loaded micelles was enhanced. This tumor acidification-induced tumor-targeting micelles significantly promoted anticancer efficacy. PBA-containing materials also can be combined with immunotherapy for tumor treatment. For example, Shi's group [37] have designed an immunomodulating nanoparticle with modification of polymer-coated BSA with PBA and immunoglobulin G, which can *in situ* activate the tumor-infiltrating natural killer cells through the interaction between PBA groups in nanoparticles and the overexpressed sialic acid in cancer cells, leading to a remarkable anticancer effect in mice.

2.2.2 Detection of tumor cells

Molecular imaging is very helpful for the early detection of diseases and can provide continuous monitoring of the progression of cancers after different treatments. Accurate analysis of the sialic acid expression in tumor cells is vital for early recognition of cancers and the estimation of cancer metastasis [38,39]. Many various PBA-incorporated materials were reported for the detection of sialic acid expressed on the cancer cells or distinguishing cancer cells from normal cells by fluorescence imaging [40–42]. Introduction of PBA group into magnetic resonance imaging (MRI) contrast agents affords sialic acid targeted MRI [43]. Recently, PBA group was conjugated to 1,4,7,10-tetraazacyclododecane-1,4,7,10-tetraacetic acid (DOTA) through a spacer of ethylenediamine (en) to form DOTA-en-PBA, which can be used to detect the overexpressed sialic acid in tumor area via MRI and PET [44,45]. As showed in Figure 5, PBA incorporated agent showed superior MRI imaging property than analogous Gd-HPDO3A (a commercial MRI agent). Additionally, Liu's group [46] has developed molecularly imprinted polymers (MIPs), which consisted of glycan imprinting PBA functionalized nanoparticles and could specifically distinguish an intact glycoprotein and its distinctive fragments. Taking advantage of the interaction between PBA and saccharide, glycans templates obtained from the digestion of target glycoprotein could immobilize onto the nanoparticles. Then, a layer of a predetermined polymer was coated on the glycans' surface. After eluting by an acidic solution, the glycans templates inserted into nanoparticles could be removed by the dissociation of boronate ester bonds, resulting in glycan-imprinted nanoparticles, which can recognize glycoproteins, glycopeptides, and glycans. Integrating PBA modified materials with surface-enhanced Raman scattering (SERS) technology, which is a non-invasive tool with high sensitivity for imaging and detection, is another effective strategy for detection and recognition of sialic acid and glycoprotein [47,48]. Sialic acid imprinted Ag @SiO_2 nanoparticles showed distinguished SERS signals for specific detection of cancer cells and tissues (Figure 5) [49]. Sialic acid imprinted core-shell particles decorated with different fluorophores were also developed for selective labeling of the sialic acid on the surface of different cell lines [50]. Similarly, Liu *et al*. [51] have prepared a kind of sialic acid imprinted nanoparticles. Comparing to non-sialic acid imprinted nanoparticles, sialic acid imprinted nanoparticles could distinguish the sialic acid overexpressed DU 145 cells and sialic acid less expressed HeLa cells via fluorescence imaging (Figure 5(f)). To achieve a high selectively imaging of cancer cells from normal cells, PBA targeting often integrated with other target agents such as somatostatin receptor and cathepsin B to obtain a dual-targeting even multitargeting imaging system [52].

2.3 Saccharides-responsive PBA-containing biomaterials

Saccharides have an important impact on life activities and abnormal metabolism of carbohydrates and are highly associated with diseases such as diabetes and cancers. Sugar-responsive biomaterials can be utilized to develop sugar-responsive insulin delivery systems, which act as artificial

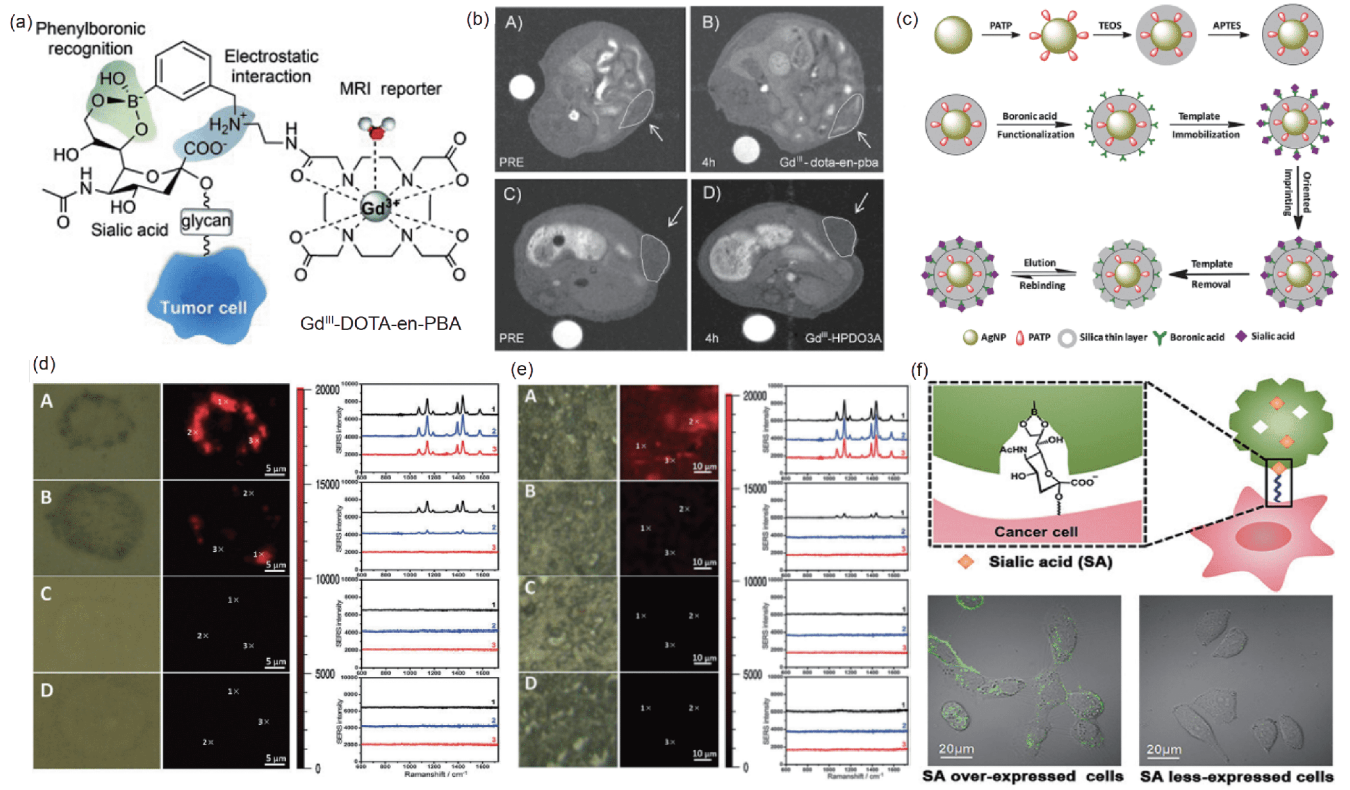

Figure 5 PBA-containing materials used for sialic acid-targeting tumor cell detection. (a) PBA incorporated MRI contrast agent was utilized for tumor cell recognition through binding to the sialic acid. (b) Fat-suppressed T1-weighted MR spin-echo images of mice bearing B16-F10 tumors administrated with Gd^{III}-DOTA-en-PBA and analogous Gd-HPDO3A, adapted with permission from Ref. [45], copyright by WILEY-VCH Verlag GmbH & Co. KGaA, Weinheim (2013). (c) Synthesis of sialic acid imprinted Ag@SiO_2 nanoparticles. SERS imaging of tumor cells (d) and tumor liver tissues (e) comparing to normal cells and normal liver tissues, adapted with permission from Ref. [49], copyright by American Chemical Society (2017). (f) Sialic acid imprinted nanoparticles applied for fluorescence imaging of sialic acid overexpressed cancer cells, adapted with permission from Ref. [51], copyright by the Royal Society of Chemistry (2017) (color online).

pancreas and can release insulin to control the blood glucose level in a normal range as it elevated [53]. On the other hand, the cancer cell surface is covered with a layer of glycans and glycoproteins, referred to as the glycocalyx, which is associated with malignancy and metastasis of tumors [54,55]. Targeting therapeutic agents to these polysaccharides may enhance intracellular drug delivery, especially for large protein drugs. PBA shows great potential in the preparation of sugar-response biomaterials since it can bind the diol structures in sugars to form dynamic boronate ester bonds (Figure 6). In an alkaline solution, PBA firstly combines with a hydroxide, exists as tetrahedral monoboronate form and then forms a cyclic ester with diol moiety in a sugar molecule. The binding constant is affected by pK_a's of sugars and PBAs and the solution pH. When PBA moiety acts as a crosslinker, the structure of nanomaterials will loose and even dissociate and then release cargos, as soon as sugars binding.

2.3.1 *Insulin delivery*

The most effective way to treat diabetes is subcutaneous injection of insulin daily. However, there are still some

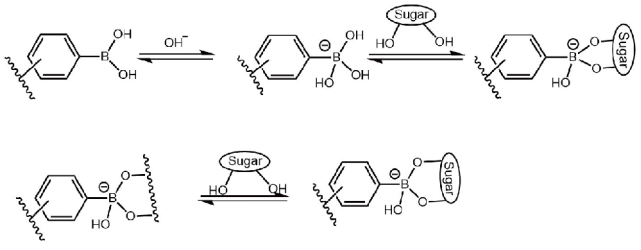

Figure 6 The sugar-binding ability of PBA-containing materials.

challenges such as patient compliance, injection doses of insulin are closely related to carbohydrate intake and activity, and hypoglycemia needs to be addressed. Designing an intelligent system that can on-demand delivery and release of insulin, similar to the pancreas, is very necessary [56]. Due to the glucose-responsive, PBA containing biomaterials can be used for insulin delivery in the diabetic therapy [57–59]. Insulin derivatives, modified with an aliphatic portion and a PBA moiety, showed long-acting and glucose-responsive abilities [60]. The introduction of fluorine, nitro, and sulfo in PBA derivatives can provide low pK_a, which could facilitate glucose-binding at physiologic pH. Gu's group have made

many efforts on the on-demand delivery of insulin and inhibition of hyperglycemia and hypoglycemia, including glucose oxidase-based glucose-sensing systems [61–63], glucose transporter inhibitor-conjugated insulin [64], and oral insulin delivery system [65]. Specifically, a PBA-containing polymer with charge reversal was designed for insulin delivery in mice and pigs and showed fast glucose-response (Figure 7) [66]. After the polymerization and subsequent deprotection of tert-butyl(2-acrylamidoethyl) carbamate (Boc-EDAA), 4-carboxy-3-fluorophenylboronic acid (FPBA) was conjugated onto the polymers, resulting in poly(EDAA0.4-FPBA0.6). The zeta potential of poly

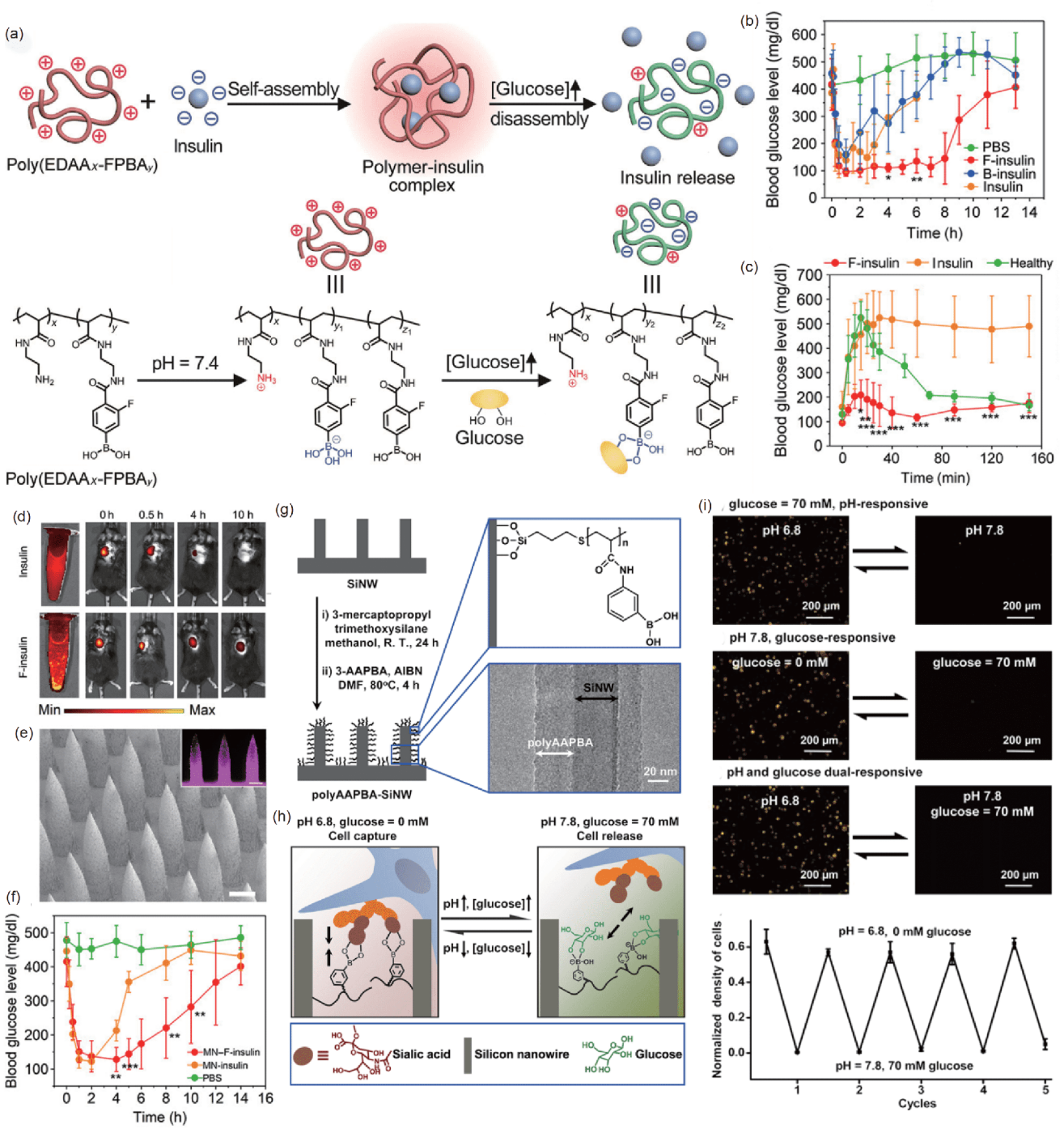

Figure 7 PBA-containing materials utilized for glucose-sensitive insulin delivery and cell capture. (a) Schematic of glucose-responsive PBA-containing biomaterials for insulin delivery. (b-f) *In vivo* evaluation of the blood glucose controlling capacity of F-insulin for type 1 diabetic mice, adapted with permission from Ref. [66], copyright by Advancement of Science (2019). (g) Synthesis and TEM image of SiNW array with a polyAAPBA brush. Illustration (h) and evaluation (i) of the pH and glucose dual-responsiveness of polyAAPBA modified SiNW, adapted with permission from Ref. [75], copyright by American Chemical Society (2013) (color online).

(EDAA0.4-FPBA0.6) was positive in phosphate buffer saline (PBS) (pH 7.4) and decreased as the glucose concentration increased in solutions. Poly(EDAA0.4-FPBA0.6) was able to load insulin as a complex (F-insulin) with high loading content and the glucose-response charge reversal was suitable for glucose-controlled insulin release. Under hyperglycemic situations, the charge of the polymer changed from positive to negative, expediting the fast release of insulin. In addition, when the blood glucose level returned to the normal range, this charge reversal was prohibited, thus decreasing the insulin release and subsequently lowering the risk of hypoglycemia. Comparing to native insulin, F-insulin can lower the blood glucose level to the normal range for about 8 h after subcutaneously injected into type 1 diabetic mice. Moreover, F-insulin can be co-injected with *in-situ* shaped gel or loaded into a microneedle array patch for *in vivo* applications. Microneedles, which have sharp needles, pave a way for subcutaneous delivering insulin and non-invasively modulating glucose levels [67,68]. Combining PBA-contained silk fibroin and acrylamide derivative, Chen *et al*. [69] reported a microneedle, which showed long-term on-demand insulin delivery. Except for microneedles, PBA-containing polymer gel is able to cooperate with other medical equipment like catheters, to provide a pancreas-like function for diabetic [70].

2.3.2 *Capture and release*

By virtue of the dynamic boronate-affinity with diol molecules, nanomaterials with surface engineered of PBA groups, are supposed to achieve selectively capture and release specific biomolecules and cells "on-demand" [71–74]. Wang and co-workers [75] have reported a pH and glucose dual-responsive surface through modification of aligned silicon nanowire (SiNW) array with a poly(acrylamidophenylboronic acid) (polyAAPBA) brush. At pH 6.8, polyAAPBA showed specific interaction with sialic acid on the tumor cells and thus could capture them. When the pH was elevated and glucose was further added, the boronate ester bonds between polyAAPBA and sialic acid would be replaced by stable binding between polyAAPBA and glucose and thus the cells would be released. This capture and release process is reversible and can be repeated for several times. Furthermore, Chen and co-workers [76] have utilized PBA-containing polymer brushes to derivatize a gold surface. A series of functional β-CD derivatives modified with various biomolecules (CD-X) can adhere to the surface of gold through the interaction between PBA and secondary hydroxyls on β-CD. Due to the dynamic characteristic of the boronate ester bonds, the CD-X molecule can be captured and released or replaced with other *cis*-diol containing biomolecules that have a higher affinity for PBA.

Taking advantage of the capture and release properties, Liu's group [77] has synthesized PBA conjugated mesoporous silica nanoparticles (MSNs) which can be applied as a nanoscale reactor. Through boronate affinity interaction, PBA functionalized MSNs initially captured target saccharides from a mixture solution. Subsequently, the labeling agents were introduced and reacted with the glycans *in situ*. The labeling reaction could be accomplished in 2 min and the reaction speed was 210-fold of that in liquid-phase labeling. The excessive reagent could be removed by simply washing with a fresh buffer, resulting in products with good purity. In addition, the labeling products could be eluted with a solution with pH<3 and regenerating the PBA functionalized MSNs for further use. Hashimoto *et al*. [78] synthesized two probes in which phenylboronic acid was conjugated with pyrene or anthracene, respectively. These PBA conjugated probes showed great potential in the detection of sugar molecules. Further, a sensor array can be designed for rapidly discriminating different ginsengs with massive diols through reversible covalent association [79].

2.3.3 *Self-healing biomaterials*

Materials bearing dynamic covalent bonds or noncovalent supramolecular interactions show self-healing capabilities and tailorable mechanical properties. Owing to their great cytocompatibility, self-healing hydrogels have been applied in various biological fields including cellular matrix, tissue engineering, and drug delivery carriers. The boronate/boronic esters structure formed between PBA and diols can dissociate reversibly in aqueous media, which have been successfully exploited for the construction of diverse self-healing materials [80–83].

For example, Anderson's group [84] synthesized an injectable hydrogel with self-healing property through the PBA-glucose complexation. Recently, Li *et al*. [85] reported a telechelic multifunctional PEG (MF-PEG) modified with PBA and benzaldehyde groups. The MF-PEG was then used to cross-link poly(vinyl alcohol) and glycol chitosan via borate ester and imine bonds, respectively, leading to a double-dynamic-network (DDN) self-healing hydrogel with heightened mechanical properties and adhesion capacity (Figure 8). The DDN hydrogels with two dynamic linkages showed self-healing and self-adapting abilities and could transform from tree-shape to star-shape with almost complete strength recovery. The excellent cytocompatibility and biosafety of the DDN hydrogels were validated in both SMMC-7721 human hepatoma cell and L929 mouse fibroblast cell. When injected under the skin of mice, the DDN hydrogels could degrade gradually and no inflammation or disease was found in the tissues around. Boroxines, which can dissociate to boronic acid under basic aqueous solution or heating, also have been applied to prepare self-healing polymers. Sun and co-authors [86] used ortho-aminomethyl-PBA to crosslink poly(propylene glycol) and obtained a polymer network with self-healing property through the

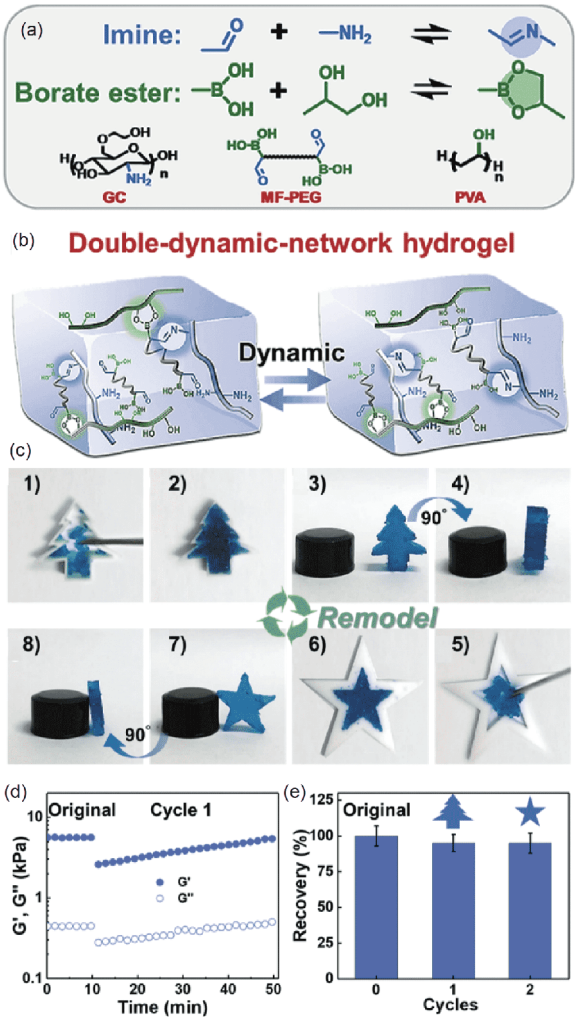

Figure 8 Hydrogels based on PBA-containing materials. (a, b) DDN hydrogels with two dynamic linkages; (c) DDN hydrogels transformed from tree shape to star shape; (d, e) G′ and G″ recovery of DDN hydrogels, adapted with permission from Ref. [85], copyright by American Chemical Society (2019) (color online).

forming of nitrogen-coordinated boroxines. By virtue of the high reversibility of nitrogen-coordinated boroxine, the cross-linked network showed distinguished self-healing property at room temperature and can be repeated several times under low pressure (0.4 kPa) without losing original mechanical strength.

2.4 N-B coordination of PBA-containing biomaterials

PBA, as a common Lewis acid, is able to form Lewis acid-base reaction with donor atoms such as nitrogen and oxygen. Although the exact nature of the boronic acid-amino base has been debated much, it is clear that this interaction shows some advantages. Firstly, this N-B interaction decreases the pK_a of PBAs, allowing them to bind diols in a neutral environment, which is very important for biological applications. Secondly, this interaction can be enhanced by the increased acidity at the boron atom after the saccharide binding [87]. The reversible and specific coordination interactions between PBAs and electron-donating groups can be utilized for crosslinking the materials and improving the drug loading capacity for electron-donating chemo-drugs.

Wang *et al*. [88] have developed BSA nanoparticles cross-linked by poly(*N*-3-acrylamidophenylboronic acid) by virtue of the coordination between PBA groups and the amines in the BSA. To illuminate such interactions, PBA with different amount of BSA was mixed in deionized water and the mixture was subsequently investigated by ^{11}B NMR. Only one peak appeared regardless of the BSA content, because the peaks of free PBA and PBA complexed with BSA were indistinguishable. Furthermore, with the increased BSA content in the mixture, the peak shifted upfield significantly and became broad gradually due to the Lewis acid-base reaction between the PBA and BSA. By virtue of the coordination between the PBA group and the amino group in DOX, a satisfactory drug loading of about 11.2% was obtained. The DOX-loaded PBA-rich BSA nanoparticles improved the liver accumulation of DOX from 15 μg/g tissue for free DOX to 40 μg/g tissue and eventually exhibited significant anticancer efficacy for mice bearing orthotopic liver tumors with a high expression level of sialic acid. Especially, a 30% reduction in the tumor size of the mice treated with this 40 nm PBA-rich drug-loaded nanoparticles was found, which was significantly different from the increasing tumor sizes of mice treated with other formulations. Polymers modification with PBA and its derivatives can improve their drug loading capacity for drugs with amines groups. Yin and co-workers [89] have synthesized an amphiphilic copolymer (named P-PBA) with pendant PBA groups on the side-chain ends of the hydrophobic segment, which showed high drug loading capacity with DOX due to the N-B coordination between DOX and PBA (Figure 9). ^{11}B NMR was used to study the interaction between DOX and PBA. For the PBA molecule, a typical chemical shift was found at 29–30 ppm. Due to the coordination between PBA and the amine of DOX, a peak at ~20 ppm appeared with or without the addition of water. The coordination of PBA with various amines was further evaluated and showed selectivity for primary, secondary and tertiary amine. DOX and epirubicin, which have primary amines, can be encapsulated into P-PBA micelles with high loading (~50%). Irinotecan with a tertiary amine can also be loaded with high capacity, but camptothecin can not be loaded due to the lack of amines in the structure. In addition, comparing to copolymer without PBA moiety (C-PBA), the hydrodynamic size of P-PBA micelles with different DOX feeding content was significantly smaller (<50 nm) than that of C-PBA micelles (>700 nm).

Cytosolic protein delivery is very important for biological medicine and protein-based therapeutics. However,

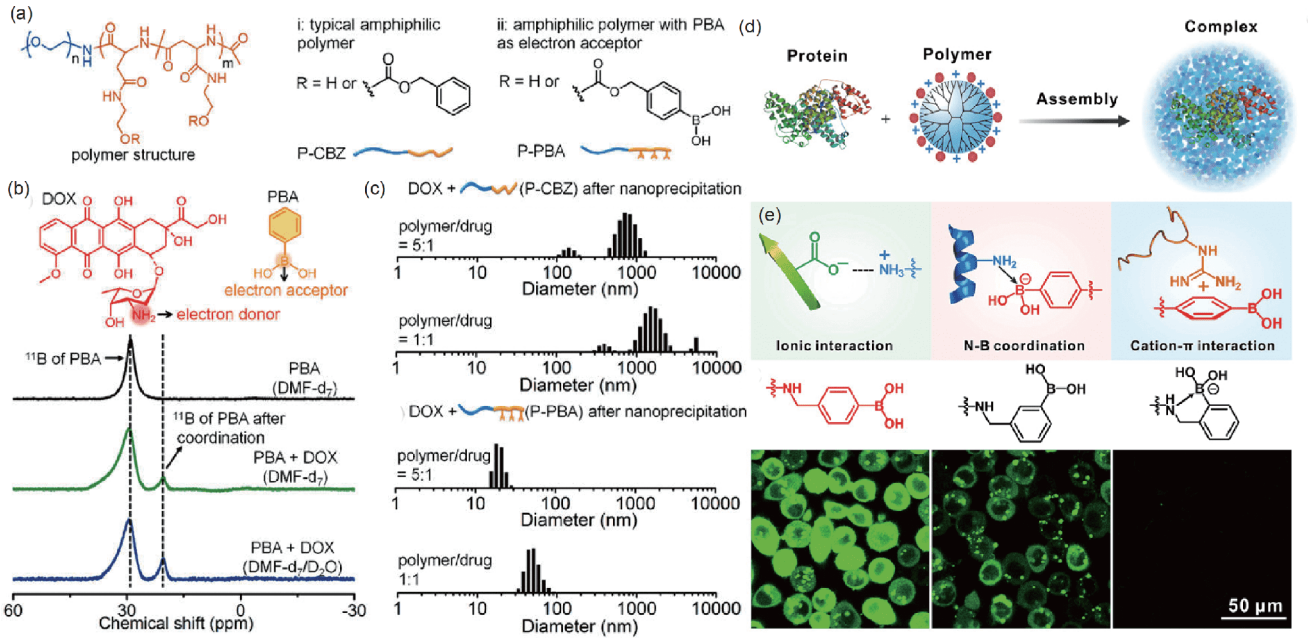

Figure 9 N-B coordination between PBA-containing materials and amines used for improving drug loading. (a) Amphiphilic copolymer with an electron acceptor was synthesized. (b) ^{11}B NMR spectra were used to verify the coordination between PBA and DOX. (c) The size distribution of different micelles loaded with different amounts of DOX, adapted with permission from Ref. [89], copyright by American Chemical Society (2018). (d) PBA-riched dendrimers complexed with proteins through a combination of N-B coordination, cation-p, and ionic interactions. (e) Dendrimers modified with different PBA derivates showed distinct protein delivery capacities, adapted with permission from Ref. [90], copyright by American Association for the Advancement of Science (2019) (color online).

efficient intracellular delivery of intact proteins by a universal approach is still a challenge since the protein activity highly depends on the structures. The larger size and the different isoelectric points are other factors that need to be considered. Cheng and co-workers [90] have synthesized a PBA-rich cationic dendrimer that is able to bind various proteins with high binding affinity through a combination of N-B coordination, cation-π, and ionic interactions and allowing efficient cytosolic delivery (Figure 9). The structure of the PBA compound used and the conjugation density on the dendrimers significantly affected the cytosolic delivery efficacy. The dendrimer conjugated with *p*-aminomethyl PBA showed superior cytosolic delivery efficacy than those conjugated with *o*-aminomethyl PBA and *m*-aminomethyl PBA. Comparing to dendrimers unmodified or conjugated with little PBA groups, the dendrimer conjugated with 60 PBA molecules showed a markedly cytosolic delivery efficacy of BSA, suggesting plenty of PBA groups in dendrimers are essential for efficient proteins delivery. Thirteen proteins with molecular weight varied from 12.4 to 430 kD and isoelectric points changed from 4.3 to 10.8, kept their bioactivities after being delivered into the cytosol by this PBA-rich dendrimer. Further, Cas9 protein was efficiently delivered into different cells by the dendrimer which revealed high efficacy in CRISPR-Cas9 genome editing.

2.5 ROS-responsive PBA-containing biomaterials

ROS overproduction is found in the inflammatory site and associated with cancer progression and metastasis [91]. ROS shows a cytotoxic effect and can lead to cell death, thus the ROS detection and depletion in inflammatory sites are particularly necessary. However, cancer cells become adapted to oxidative stress [92]. In cancer cells, the overexpressed ROS can be used to selectively induce drug release. For example, drug delivery systems with ROS-liable drug release could be designed to enhance their antitumor efficacy and reduce toxicity in normal tissues. The reaction between hydrogen peroxide (H_2O_2) and PBA has been regarded as the basis of H_2O_2-selective probes, ROS-liable drug release, and prodrug strategies.

2.5.1 ROS-responsive drug delivery

H_2O_2 produced in living organisms has an ability to kill cells and play important roles in cellular signaling, but an overproduction of H_2O_2 is highly associated with inflammation in injury, and diseases. Due to the stoichiometric consumption of H_2O_2, PBA and its derivatives are widely used to modify materials to afford H_2O_2-responsive ability [93]. For instance, He *et al*. [94] modified RNase A with PBA to form an H_2O_2-cleavable prodrug. Under light irradiation, hematoporphyrin in the system could generate high levels of H_2O_2

that facilitates the complete recovery of protein activity of RNase A by cleaving the PBA group. Owing to the vigorous metabolic activation, the ROS production increased and the pH values lowed in inflammatory regions comparing to normal tissues. PBA modified materials with ROS and pH dual-responsive ability are suitable carriers for anti-inflammatory drug delivery [95]. Hoang *et al*. [96] conjugated angiogenin (ANG) with PBA through a thiol-ene reaction between the inserted cysteine in ANG and the allyl in PBA (Figure 10). The reactivity of ANG was cloaked at normal physiological conditions and recovered in the presence of ROS, making the PBA conjugated ANG suitable for target-

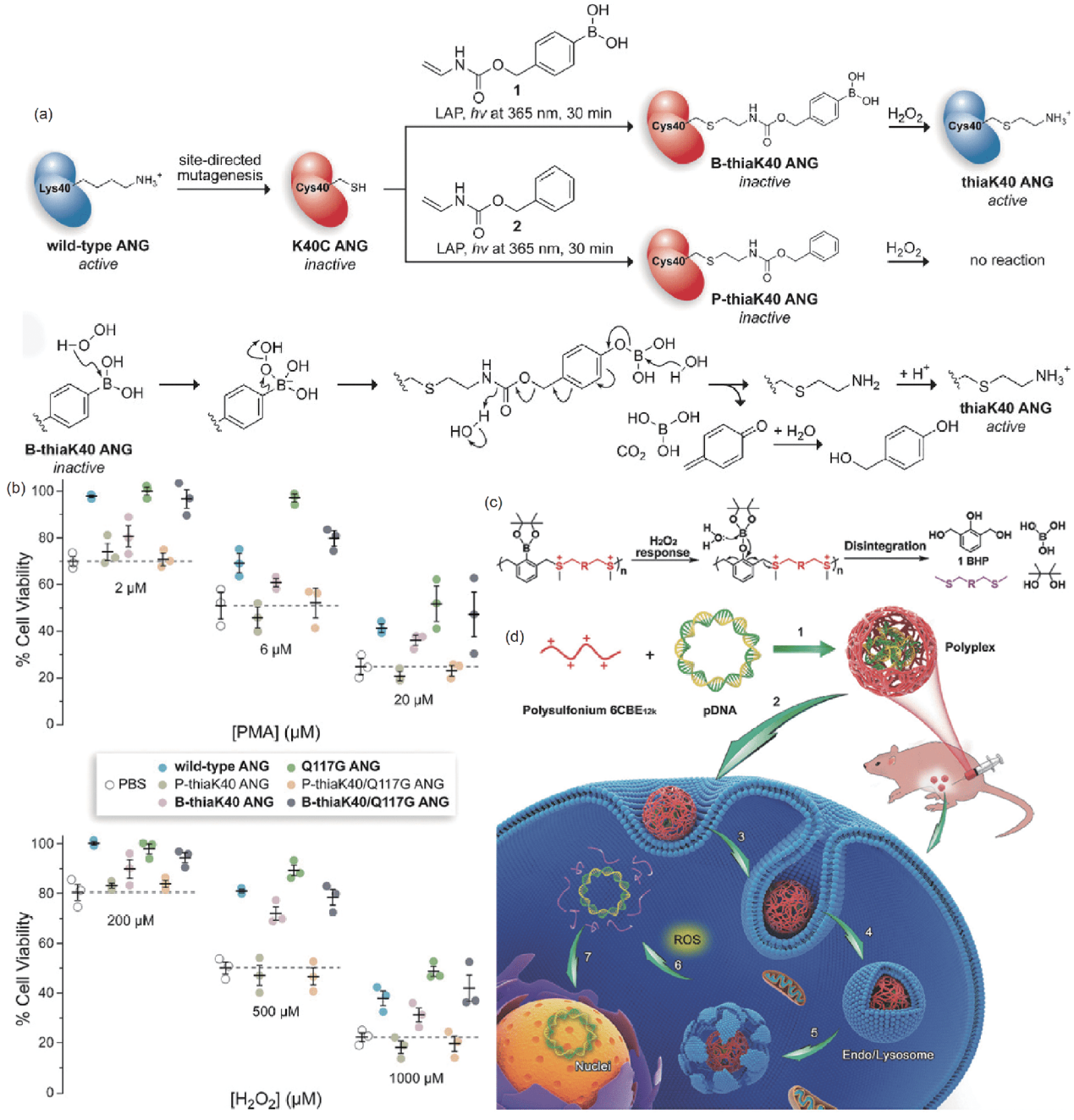

Figure 10 H_2O_2-responsive of PBA-containing materials applied in the biomedical area. (a) Masking of the active site in human ANG through a ROS-responsive PBA group. The biological activity of ANG can be recovered under high levels of H_2O_2. The expected mechanism of H_2O_2-responsive cleavage of the PBA residue. (b) The cell viability of human astrocytes treated with different ANG molecules before exposure to different amounts of PMA and H_2O_2, adapted with permission from Ref. [96], copyright by Wiley-VCH Verlag GmbH & Co. KGaA, Weinheim (2017). (c) The proposed mechanism of ROS-induced disintegration of polysulfonium. (d) The ROS-sensitive polysulfonium can be utilized to complex pDNA and achieving ROS-triggered release once internalized in tumors, adapted with permission from Ref. [101], copyright by WILEY-VCH Verlag GmbH & Co. KGaA, Weinheim (2017) (color online).

ing therapy for amyotrophic lateral sclerosis (ALS), which is associated with the high accumulation of H_2O_2. Pretreatment of human astrocytes with PBA-masking ANG protects them from subsequent oxidative stress from phorbol 12-myristate 13-acetate (PMA) and H_2O_2. And the bioactivity of ANG recovered from PBA-masking ANG was similar to that of wild-type ANG, suggesting the ROS-responsive recovery of bioactivity of PBA-masking ANG. PBA moieties in materials also afford opportunities for the cytosolic delivery of gene drugs [97,98].

Shen's group [99,100] has explored many methods on the preparation of ROS-responsive polymers for gene delivery through PBA-containing cationic polymers. For example, polysulfonium modified with PBA groups was synthesized and it could be degraded when exposure to a high level of H_2O_2. This polysulfonium condensed plasmid DNA into polyplexes with ROS-induced pDNA release [101]. After cellular internalization, the overexpressed ROS could disintegrate the polyplex and release the loaded DNA molecules. Shi's group [102] have developed pH and H_2O_2 dual-responsive nanoparticles through the complexation of 4-(hydroxymethyl) phenylboronic acid (HPBA)-modified polyethyleneimine with plasmid DNA encoding the CRISPR/Cas13a system, following coating of *cis*-aconitic anhydride and sodium glucoheptonate dehydrate-modified poly(ethylene glycol)-*b*-polylysine (mPEG-pLys-CA/SGD) through the interaction between PBA and SGD. Upon low pH and high concentration of H_2O_2 in the tumor site, the outside mPEG-pLys-CA/SGD coating splits, releasing the CRISPR/Cas13a polyplex and thus enhancing the cancer immunotherapy through disruption of the PD-1/PD-L1 pathway. The photosensitizer (PS) could be involved to produce exogenous ROS to improve ROS-responsiveness. Yin and co-workers [94] caged RNase A in a nanocarrier through a ROS-responsive PBA-containing material. With 635 nm light irradiation, ROS were generated by PS, thus the nanocarrier disassembled and released the caged RNase A.

2.5.2 Detection of ROS

ROS detection is important for monitoring inflammation development and PBA-containing materials offer opportunities for this [103,104]. Chang and co-workers [105] have reported a chemoselective bioluminescent probe, peroxy caged luciferin-1 (PCL-1), for the real-time detection of H_2O_2 *in vivo*. The H_2O_2-responsive PBA was conjugated with firefly luciferin via a self-immolative linker. In the presence of high concentration H_2O_2, the linker could be cleaved and release the luciferin, resulting in an H_2O_2-sensitive probe. Almutairi and co-workers [106] have developed a nanoprobe with ROS and pH dual-responsive abilities, consist of a PBA-modified dextran and an acetylated dextran. This nanoprobe is enabled to distinguish inflamed areas with a high target-to-background ratio of about 22 as early as 3 h after administration. This H_2O_2-responsiveness can also induce the structural transitions of different assembly nanoarchitectures [107].

2.6 ATP-responsive PBA-containing materials

ATP plays a crucial role in a range of biological processes such as energy-dependent metabolism and signaling. The intracellular concentration (1–10 mM) of ATP is significantly higher than that in the extracellular environment (<5 μM), suggesting that ATP can be a stimulus for the intracellular release of cargos [108,109]. For example, Qian *et al*. [110] have reported a 3-fluoro-4-carboxyphenylboronic acid-modified conjugated polymer as a nanocarrier to deliver DOX into cancer cells. Through binding with overexpressed sialic acid on tumor cells, the nanocarriers achieved tumor-specific accumulation. After internalization into cancer cells, the PBA groups in nanocarriers could interact with a high concentration of ATP in the cells, leading to the dissociation of nanocarriers and drug release.

A supramolecular assembly with ATP-trigged dissociation and siRNA release behaviors have been reported [111]. The supramolecular assembly formed via host-guest interaction between polyethyleneimine (PEI) 1.8k-α-cyclodextrin (α-CD) conjugates and PEI1.8k-phenylboronic acid (PBA) conjugates, which were utilized as siRNA delivery carriers. After internalized into cells, the assembly fell apart gradually and siRNA released in response to intracellular ATP with high concentration. Polyplex micelles from cationic copolymers modified with 4-carboxy-3-fluorophenylboronic acid (FPBA) and D-gluconamide with crosslinked cores were prepared by Kataoka and co-workers [112] and further applied for ATP-responsive intracellular delivery of plasmid DNA. Sun's group [113] synthesized a PBA containing crosslinked polymer with strongly positively charged, which could package siRNA effectively and became degraded and charger reversed once expose to the intracellular concentration ATP. To improve the serum stability, ATP-grafted hyaluronic acid was used to crosslink polyplexes through a reversible covalent between ATP and PBA conjugated onto PEI (Figure 11) [114]. This HA-PEI/siRNA complex with covalent crosslinking showed great luciferase silence in B16F10-Luc tumor-bearing mice comparing to the complex with non-covalent crosslinking.

PBA-containing materials with ATP-responsive property also have been used to develop ATP sensors [115]. Self-assembled sensors based on ZnII-dipicolylamine-attached to PBA were developed [116]. In the presence of phosphates including PPi, ATP, and AMP, these sensors exhibited different color diversity that enables quantitative assessment of the phosphate concentrations and resulting in an ATP-detection probe, which could achieve the specific detection of

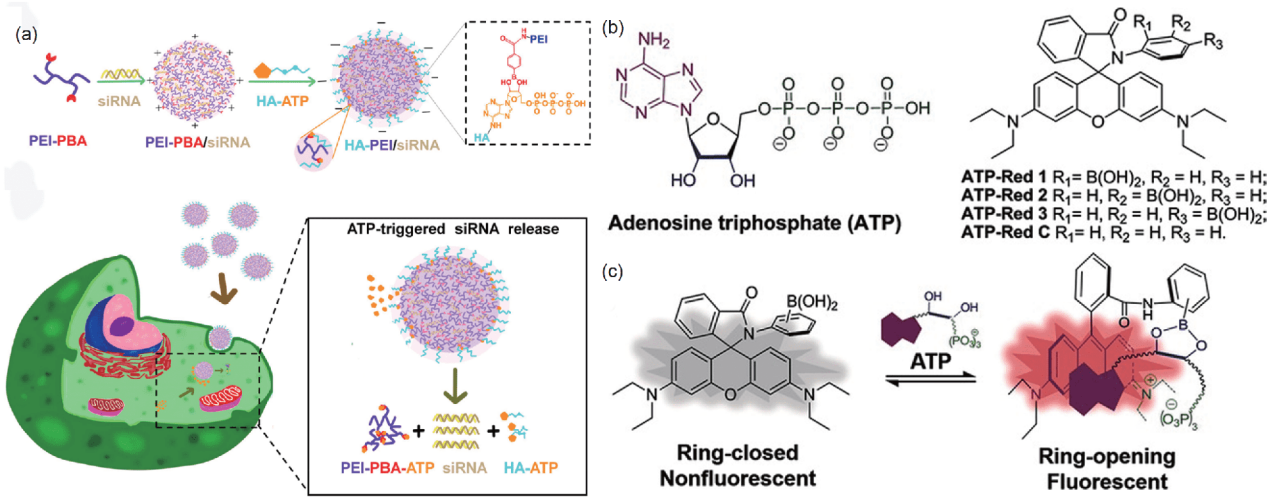

Figure 11 ATP-sensitive PBA-containing materials applied in the biomedical area. (a) Synthesis of HA-PEI/siRNA complex with ATP-triggered siRNA release, adapted with permission from Ref. [114], copyright by American Chemical Society (2018). Structure of ATP-sensing probes (b) and the putative mechanism (c), adapted with permission from Ref. [117], copyright by WILEY-VCH Verlag GmbH & Co. KGaA, Weinheim (2016) (color online).

ATP through multiple interactions including covalent bonding between boronic acid and ribose, π-π interactions between xanthene and adenine, and electronic attraction between amino and phosphate groups (Figure 11) [117]. When rhodamine B was linked at ortho-position, the obtained probe ATP-Red 1 showed a strong fluorescence response to ATP at intracellular concentrations.

2.7 Dopamine-responsive PBA-containing materials

Dopamine, which has a catechol structure, also can form dynamic covalent bonds with PBAs. As a neurotransmitter, dopamine regulates multiple physiological functions of the central nervous system. Boronic acid derivatives can be introduced into various probes and nanomaterials for dopamine detection [118,119]. Shen's group [120] introduced PBA groups into conjugated polymer nanoparticles to image the amount change of dopamine in living cells, zebrafish and mice. The PBA-containing conjugated polymer showed high-sensitivity for dopamine detection both *in vitro* and *in vivo*. Further, the conjugated polymers were applied for analyzing the neural activity in alcohol-activated mice via imaging the dopamine-producing in brains [121].

2.8 Nuclear-targeting PBA-containing nanobiomaterials

Nuclear targeting drug delivery is of much importance in disease therapy, especially in cancer therapy, since lots of anti-cancer drugs including DOX, camptothecin, and *cis*-platin, need to bind nuclear DNA or enzymes to exert their functions. Most of the traditional drug delivery systems concern cytoplasmic delivery and the loaded drugs need to be released in the cytoplasm and subsequently entered into the nucleus through diffusion. Since they can deliver drugs into the nucleus directly, nuclear targeting drug delivery systems are attracting much attention [122]. A variety of strategies have been developed for the nuclear targeting drug delivery system such as cationic poly(L-lysine) modification [123], cell penetration peptide conjugation [124,125], photodynamic assistance [126,127]. However, achieving effective nuclear delivery still remains a challenge, especially for proteins with large size, which is hard to transport the nupores through passive pathways.

Tang *et al.* [128] reported that benzyl boronate (BB) conjugation drove the nuclear targeting delivery of proteins through active transportation pathway as shown in Figure 12. Comparing to benzyl modified green fluorescent protein (GFP-B), a large amount of PBA modified green fluorescent protein (GFP-BB) accumulated in the cellular nucleus after intracellular delivery using gold nanoparticles stabilized capsules (NPSCs). When cells were pretreated with ivermectin to block the importin α/β pathway or the ATP in HeLa cells was depleted, the nuclear accumulation of GFP-BB was highly decreased, suggesting the PBA mediated nuclear targeting was energy-dependent and mainly regulated by the importin α/β pathway through the binding of GFP-BB with importin. Pan and coworkers [129] further used catechol-borane interaction to modify the carbon nanodot, resulting in an ultrafine-sized nanocarrier with nuclear target ability. The dynamic covalent network formed through boronic ester bonds of the interaction between catechol groups and boronic acid groups, would dissociate at the weak acid tumor environment and resulting in the exposure of PBA groups to bind glucosamine presented at nucleoporin 62 (NUP62) and thus targeting nucleus. After incubation for 4 h, all the nanocarriers were located in the nucleus.

3 Conclusions and outlook

In summary, PBA-containing biomaterials have many advantageous features, such as sialic acid-binding, sugar-binding, ROS-responsive, pH-responsive, ATP-responsive, dopamine-responsive and nuclear-targeting. They also be able to bind with other glycols, showing great potential in a wide range of biomedical applications such as drug delivery, cell and tumor imaging, sensors and detections, and self-healing. PBA shows a high associated constant with sialic acid especially in a weak acid environment, which is suitable for application in the tumor microenvironment, where the pH is usually about 6.5. Besides, PBA containing biomaterials can bind saccharides through boronate ester bonds, allowing for sugar detection in a physiological environment. In general, the introduction of electron-withdrawing groups could reduce the pK_a of PBA, and then reduce the optimal pH for binding to sugar molecules. Due to the interaction between PBA and the diol groups in siRNA and the N-B coordination between PBA and amines, PBA containing materials showed high drug loading capacity for siRNA and electron-donating chemo-drugs. The high concentration of ATP and ROS in diseased cells could subsequently stimulate the drug-loaded nanocarriers' dissociation and release drugs. We also review the PBA containing biomaterials applied as sensors for the detection of sialic acid, glucose, ATP *in vitro*. The exclusive property of PBAs to bind to diol-molecules reversibly at physiologic pH endows the further development of self-healing materials. The major PBA-containing biomaterials mentioned in this review for biomedical applications were summarized in Table 1.

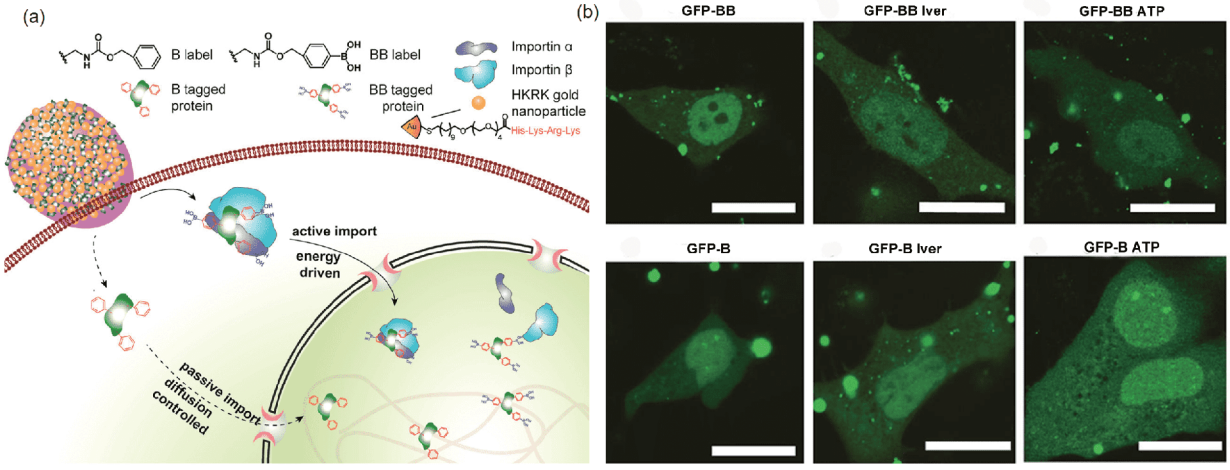

Figure 12 The nuclear targeting ability of PBA-containing materials. (a) The nuclear targeting delivery of proteins with BB conjugation after intracellular delivery by NPSCs. (b) The nucleus targeting the ability of GFP-BB and GFP-B in HeLa cells with or without pretreatment with ivermectin or ATP depletion, evaluated by CLSM imaging, adapted with permission from Ref. [128], copyright by American Chemical Society (2017) (color online).

Table 1 Summary of the major PBA-containing biomaterials mentioned in this review for biomedical applications

Responsiveness	Biomolecules	Applications	Refs.
Sialic acid-binding	Sialic acid	Tumor targeting drug delivery	[29–32, 35,36,88]
		Detection of tumor cells	[43–46, 49–51]
Sugars-responsive	Saccharides	Insulin delivery	[60,66,69,70]
		Capture and release	[75–77]
		Self-healing materials	[84–86]
N-B coordination	Amines	High drug loading for drug delivery	[89,90]
ROS-responsive	H_2O_2	ROS-responsive drug delivery	[94–96, 102]
		Detection of H_2O_2	[105–107]
ATP-responsive	ATP	ATP-responsive drug delivery	[110–112, 114]
		Detection of ATP	[115–117]
Dopamine-responsive	Dopamine	Detection of dopamine	[120,121]
Nuclear targeting	Importin	Drug delivery	[128]
	Nucleoporin 62	Drug delivery	[129]

There are still many applications for PBA containing biomaterials that remain to be explored. Glycans regulate a wealth of bioprocesses essential for cell differentiation, migration, invasion, metabolic and gene regulation. ROS involved in many cellular signaling and associated with inflammation-related diseases. Further, inflammation and immunity are closely related. ATP is the most energy resource and involved in the metabolism of fats, proteins, sugars, nucleic acids, and nucleotides. Through interaction with these biomolecules, PBA-containing biomaterials can be involved in and put an impact on many bioprocesses. Glycans especially glycoproteins play vital roles in immune reactions and are becoming drug targets for immunotherapy. ROS is the main mediator of phagocytic effects and highly associated with an oxidative stress response. It is possible that PBA containing biomaterials are applied with immunotherapy through modulating the tumor immune microenvironments. On the other hand, there are also many challenges. The physiological environment is very complicated and the biomolecules mentioned above are usually involved in many different bioprocesses. Multifunctional PBA-containing biomaterials are desirable since single materials can not achieve a satisfactory outcome. Multitargeting is mostly used in tumor treatment and screening targets that can cooperate with each other are very important and not easy. Also, the rational precise control of the ratios between the different components is very difficult. On the other hand, it is hard to determine the underlying mechanism since PBA can react with many biological molecules.

Acknowledgements This work was supported by the National Key Research and Development Program of China (2017YFA0701301, 2017YFA0205400), the National Natural Science Foundation of China (51690153, 21720102005, 51803089), and the Program for Changjiang Scholars and Innovative Research Team in University and the Fundamental Research Funds for the Central Universities.

Conflict of interest The authors declare that they have no conflict of interest.

1 Brooks WLA, Sumerlin BS. *Chem Rev*, 2016, 116: 1375–1397
2 Guo Z, Shin I, Yoon J. *Chem Commun*, 2012, 48: 5956–5967
3 Ghebregzabher M, Rufini S, Sapia GM, Lato M. *J Chromatogr A*, 1979, 180: 1–16
4 Büll C, Stoel MA, den Brok MH, Adema GJ. *Cancer Res*, 2014, 74: 3199–3204
5 Gorrini C, Harris IS, Mak TW. *Nat Rev Drug Discov*, 2013, 12: 931–947
6 Di Virgilio F, Sarti AC, Falzoni S, De Marchi E, Adinolfi E. *Nat Rev Cancer*, 2018, 18: 601–618
7 Berke JD. *Nat Neurosci*, 2018, 21: 787–793
8 Wang J, Wu W, Jiang X. *Nanomedicine*, 2015, 10: 1149–1163
9 Jiang XC, Xiang JJ, Wu HH, Zhang TY, Zhang DP, Xu QH, Huang XL, Kong XL, Sun JH, Hu YL, Li K, Tabata Y, Shen YQ, Gao JQ. *Adv Mater*, 2019, 31: 1807591
10 Sun X, Xu Q, Kim G, Flower SE, Lowe JP, Yoon J, Fossey JS, Qian X, Bull SD, James TD. *Chem Sci*, 2014, 5: 3368–3373
11 Zhao L, Xiao C, Wang L, Gai G, Ding J. *Chem Commun*, 2016, 52: 7633–7652
12 Ma R, Shi L. *Polym Chem*, 2014, 5: 1503–1518
13 Guan Y, Zhang Y. *Chem Soc Rev*, 2013, 42: 8106–8121
14 Shinde S, El-Schich Z, Malakpour A, Wan W, Dizeyi N, Mohammadi R, Rurack K, Gjörloff Wingren A, Sellergren B. *J Am Chem Soc*, 2015, 137: 13908–13912
15 Kim J, Lee YM, Kim H, Park D, Kim J, Kim WJ. *Biomaterials*, 2016, 75: 102–111
16 Naito M, Ishii T, Matsumoto A, Miyata K, Miyahara Y, Kataoka K. *Angew Chem Int Ed*, 2012, 51: 10751–10755
17 Yan J, Springsteen G, Deeter S, Wang B. *Tetrahedron*, 2004, 60: 11205–11209
18 Ellis GA, Palte MJ, Raines RT. *J Am Chem Soc*, 2012, 134: 3631–3634
19 Adamczyk B, Tharmalingam T, Rudd PM. *Biochim Biophys Acta*, 2012, 1820: 1347–1353
20 Pearce OMT, Läubli H. *Glycobiology*, 2015, 26: 111–128
21 Whited J, Zhang X, Nie H, Wang D, Li Y, Sun XL. *ACS Chem Biol*, 2018, 13: 2364–2374
22 Christiansen MN, Chik J, Lee L, Anugraham M, Abrahams JL, Packer NH. *Proteomics*, 2014, 14: 525–546
23 Otsuka H, Uchimura E, Koshino H, Okano T, Kataoka K. *J Am Chem Soc*, 2003, 125: 3493–3502
24 Lei L, Xu Z, Hu X, Lai Y, Xu J, Hou B, Wang Y, Yu H, Tian Y, Zhang W. *Small*, 2019, 15: 1900157
25 Liu M, Tang X, Ding J, Liu M, Zhao B, Deng Y, Song Y. *Pharm Res*, 2019, 36: 176
26 Lee JY, Chung SJ, Cho HJ, Kim DD. *Adv Funct Mater*, 2015, 25: 3705–3717
27 Wang X, Zhen X, Wang J, Zhang J, Wu W, Jiang X. *Biomaterials*, 2013, 34: 4667–4679
28 Wang J, Wu W, Zhang Y, Wang X, Qian H, Liu B, Jiang X. *Biomaterials*, 2014, 35: 866–878
29 Wang X, Tang H, Wang C, Zhang J, Wu W, Jiang X. *Theranostics*, 2016, 6: 1378–1392
30 Chen W, Ji S, Qian X, Zhang Y, Li C, Wu W, Wang F, Jiang X. *Polym Chem*, 2017, 8: 2105–2114
31 Zhang Y, Chen W, Yang C, Fan Q, Wu W, Jiang X. *J Control Release*, 2016, 237: 115–124
32 Qian X, Ge L, Yuan K, Li C, Zhen X, Cai W, Cheng R, Jiang X. *Theranostics*, 2019, 9: 7417–7430
33 Liu S, Pan J, Liu J, Ma Y, Qiu F, Mei L, Zeng X, Pan G. *Small*, 2018, 14: 1703968
34 Obuobi S, Voo ZX, Low MW, Czarny B, Selvarajan V, Ibrahim NL, Yang YY, Ee PLR. *Adv Healthc Mater*, 2018, 7: 1701388
35 Long Y, Lu Z, Mei L, Li M, Ren K, Wang X, Tang J, Zhang Z, He Q. *Adv Sci*, 2018, 5: 1800229
36 Cao J, Gao X, Cheng M, Niu X, Li X, Zhang Y, Liu Y, Wang W, Yuan Z. *Nano Lett*, 2019, 19: 1665–1674
37 Zheng C, Wang Q, Wang Y, Zhao X, Gao K, Liu Q, Zhao Y, Zhang Z, Zheng Y, Cao J, Chen H, Shi L, Kang C, Liu Y, Lu Y. *Adv Mater*, 2019, 31: 1902542
38 Matsumoto A, Sato N, Kataoka K, Miyahara Y. *J Am Chem Soc*, 2009, 131: 12022–12023
39 Matsumoto A, Cabral H, Sato N, Kataoka K, Miyahara Y. *Angew Chem Int Ed*, 2010, 49: 5494–5497
40 Cheng L, Zhang X, Zhang Z, Chen H, Zhang S, Kong J. *Talanta*, 2013, 115: 823–829
41 Qian R, Ding L, Yan L, Ju H. *Anal Chim Acta*, 2015, 894: 85–90
42 Liu HW, Law WHT, Lee LCC, Lau JCW, Lo KKW. *Chem Asian J*, 2017, 12: 1545–1556
43 Frullano L, Rohovec J, Aime S, Maschmeyer T, Prata MI, de Lima JJP, Geraldes CFGC, Peters JA. *Chem Eur J*, 2004, 10: 5205–5217
44 Tsoukalas C, Geninatti-Crich S, Gaitanis A, Tsotakos T, Paravatou-Petsotas M, Aime S, Jiménez-Juárez R, Anagnostopoulos CD, Djanashvili K, Bouziotis P. *Mol Imag Biol*, 2018, 20: 798–807
45 Geninatti Crich S, Alberti D, Szabo I, Aime S, Djanashvili K. *Angew Chem Int Ed*, 2013, 52: 1161–1164

46 Bie Z, Chen Y, Ye J, Wang S, Liu Z. *Angew Chem Int Ed*, 2015, 54: 10211–10215
47 Ye J, Chen Y, Liu Z. *Angew Chem Int Ed*, 2014, 53: 10386–10389
48 Di H, Liu H, Li M, Li J, Liu D. *Anal Chem*, 2017, 89: 5874–5881
49 Yin D, Wang S, He Y, Liu J, Zhou M, Ouyang J, Liu B, Chen HY, Liu Z. *Chem Commun*, 2015, 51: 17696–17699
50 Wang S, Yin D, Wang W, Shen X, Zhu JJ, Chen HY, Liu Z. *Sci Rep*, 2016, 6: 22757
51 Liu R, Cui Q, Wang C, Wang X, Yang Y, Li L. *ACS Appl Mater Interfaces*, 2017, 9: 3006–3015
52 Li H, Lee CH, Shin I. *Org Lett*, 2019, 21: 4628–4631
53 Zaykov AN, Mayer JP, DiMarchi RD. *Nat Rev Drug Discov*, 2016, 15: 425–439
54 Paszek MJ, DuFort CC, Rossier O, Bainer R, Mouw JK, Godula K, Hudak JE, Lakins JN, Wijekoon AC, Cassereau L, Rubashkin MG, Magbanua MJ, Thorn KS, Davidson MW, Rugo HS, Park JW, Hammer DA, Giannone G, Bertozzi CR, Weaver VM. *Nature*, 2014, 511: 319–325
55 Tarbell JM, Cancel LM. *J Intern Med*, 2016, 280: 97–113
56 Wang J, Wang Z, Yu J, Kahkoska AR, Buse JB, Gu Z. *Adv Mater*, 2019, 1902004
57 Hou L, Zheng Y, Wang Y, Hu Y, Shi J, Liu Q, Zhang H, Zhang Z. *ACS Appl Mater Interfaces*, 2018, 10: 21927–21938
58 Xiao Y, Hu Y, Du J. *Mater Horiz*, 2019, 6: 2047–2055
59 Li C, Huang F, Liu Y, Lv J, Wu G, Liu Y, Ma R, An Y, Shi L. *Langmuir*, 2018, 34: 12116–12125
60 Chou DHC, Webber MJ, Tang BC, Lin AB, Thapa LS, Deng D, Truong JV, Cortinas AB, Langer R, Anderson DG. *Proc Natl Acad Sci USA*, 2015, 112: 2401–2406
61 Yu J, Qian C, Zhang Y, Cui Z, Zhu Y, Shen Q, Ligler FS, Buse JB, Gu Z. *Nano Lett*, 2017, 17: 733–739
62 Hu X, Yu J, Qian C, Lu Y, Kahkoska AR, Xie Z, Jing X, Buse JB, Gu Z. *ACS Nano*, 2017, 11: 613–620
63 Chen Z, Wang J, Sun W, Archibong E, Kahkoska AR, Zhang X, Lu Y, Ligler FS, Buse JB, Gu Z. *Nat Chem Biol*, 2018, 14: 86–93
64 Wang J, Yu J, Zhang Y, Kahkoska AR, Wang Z, Fang J, Whitelegge JP, Li S, Buse JB, Gu Z. *Proc Natl Acad Sci USA*, 2019, 116: 10744–10748
65 Yu J, Zhang Y, Wang J, Wen D, Kahkoska AR, Buse JB, Gu Z. *Nano Res*, 2019, 12: 1539–1545
66 Wang J, Yu J, Zhang Y, Zhang X, Kahkoska AR, Chen G, Wang Z, Sun W, Cai L, Chen Z, Qian C, Shen Q, Khademhosseini A, Buse JB, Gu Z. *Sci Adv*, 2019, 5: eaaw4357
67 Jin X, Zhu DD, Chen BZ, Ashfaq M, Guo XD. *Adv Drug Deliver Rev*, 2018, 127: 119–137
68 Wang J, Ye Y, Yu J, Kahkoska AR, Zhang X, Wang C, Sun W, Corder RD, Chen Z, Khan SA, Buse JB, Gu Z. *ACS Nano*, 2018, 12: 2466–2473
69 Chen S, Matsumoto H, Moro-oka Y, Tanaka M, Miyahara Y, Suganami T, Matsumoto A. *ACS Biomater Sci Eng*, 2019, 5: 5781–5789
70 Matsumoto A, Tanaka M, Matsumoto H, Ochi K, Moro-Oka Y, Kuwata H, Yamada H, Shirakawa I, Miyazawa T, Ishii H, Kataoka K, Ogawa Y, Miyahara Y, Suganami T. *Sci Adv*, 2017, 3: eaaq0723
71 Dong Y, Lu X, Wang P, Liu W, Zhang S, Wu Z, Chen H. *J Mater Chem B*, 2018, 6: 6744–6751
72 Shen MY, Chen JF, Luo CH, Lee S, Li CH, Yang YL, Tsai YH, Ho BC, Bao LR, Lee TJ, Jan YJ, Zhu YZ, Cheng S, Feng FY, Chen P, Hou S, Agopian V, Hsiao YS, Tseng HR, Posadas EM, Yu HH. *Adv Healthc Mater*, 2018, 7: 1700701
73 Liu L, Tian X, Ma Y, Duan Y, Zhao X, Pan G. *Angew Chem Int Ed*, 2018, 57: 7878–7882
74 Pan G, Guo B, Ma Y, Cui W, He F, Li B, Yang H, Shea KJ. *J Am Chem Soc*, 2014, 136: 6203–6206
75 Liu H, Li Y, Sun K, Fan J, Zhang P, Meng J, Wang S, Jiang L. *J Am Chem Soc*, 2013, 135: 7603–7609
76 Zhan W, Qu Y, Wei T, Hu C, Pan Y, Yu Q, Chen H. *ACS Appl Mater Interfaces*, 2018, 10: 10647–10655
77 Pan X, Chen Y, Zhao P, Li D, Liu Z. *Angew Chem Int Ed*, 2015, 54: 6173–6176
78 Hashimoto T, Kumai M, Maeda M, Miyoshi K, Tsuchido Y, Fujiwara S, Hayashita T. *Front Chem Sci Eng*, 2020, 14: 53–60
79 Pan Y, Yang M, Zhang M, Jia M. *Sens Actuat B-Chem*, 2019, 294: 48–54
80 Ma D, Wu X, Wang Y, Liao H, Wan P, Zhang L. *ACS Appl Mater Interfaces*, 2019, 11: 41701–41709
81 Bao C, Guo Z, Sun H, Sun J. *ACS Appl Mater Interfaces*, 2019, 11: 9478–9486
82 Yesilyurt V, Webber MJ, Appel EA, Godwin C, Langer R, Anderson DG. *Adv Mater*, 2016, 28: 86–91
83 Zhi X, Zheng C, Xiong J, Li J, Zhao C, Shi L, Zhang Z. *Langmuir*, 2018, 34: 12914–12923
84 Dong Y, Wang W, Veiseh O, Appel EA, Xue K, Webber MJ, Tang BC, Yang XW, Weir GC, Langer R, Anderson DG. *Langmuir*, 2016, 32: 8743–8747
85 Li Y, Yang L, Zeng Y, Wu Y, Wei Y, Tao L. *Chem Mater*, 2019, 31: 5576–5583
86 Bao C, Jiang YJ, Zhang H, Lu X, Sun J. *Adv Funct Mater*, 2018, 28: 1800560
87 Nishiyabu R, Kubo Y, James TD, Fossey JS. *Chem Commun*, 2011, 47: 1124–1150
88 Wang J, Zhang Z, Wang X, Wu W, Jiang X. *J Control Release*, 2013, 168: 1–9
89 Lv S, Wu Y, Cai K, He H, Li Y, Lan M, Chen X, Cheng J, Yin L. *J Am Chem Soc*, 2018, 140: 1235–1238
90 Liu C, Wan T, Wang H, Zhang S, Ping Y, Cheng Y. *Sci Adv*, 2019, 5: eaaw8922
91 Ishikawa K, Takenaga K, Akimoto M, Koshikawa N, Yamaguchi A, Imanishi H, Nakada K, Honma Y, Hayashi JI. *Science*, 2008, 320: 661–664
92 Trachootham D, Alexandre J, Huang P. *Nat Rev Drug Discov*, 2009, 8: 579–591
93 Song CC, Ji R, Du FS, Liang DH, Li ZC. *ACS Macro Lett*, 2013, 2: 273–277
94 He H, Chen Y, Li Y, Song Z, Zhong Y, Zhu R, Cheng J, Yin L. *Adv Funct Mater*, 2018, 28: 1706710
95 Lee S, Stubelius A, Hamelmann N, Tran V, Almutairi A. *ACS Appl Mater Interfaces*, 2018, 10: 40378–40387
96 Hoang TT, Smith TP, Raines RT. *Angew Chem Int Ed*, 2017, 56: 2619–2622
97 Liu C, Shao N, Wang Y, Cheng Y. *Adv Healthc Mater*, 2016, 5: 584–592
98 Piest M, Engbersen JFJ. *J Control Release*, 2011, 155: 331–340
99 Liu X, Xiang J, Zhu D, Jiang L, Zhou Z, Tang J, Liu X, Huang Y, Shen Y. *Adv Mater*, 2016, 28: 1743–1752
100 Xiang J, Liu X, Zhou Z, Zhu D, Zhou Q, Piao Y, Jiang L, Tang J, Liu X, Shen Y. *ACS Appl Mater Interfaces*, 2018, 10: 43352–43362
101 Zhu D, Yan H, Liu X, Xiang J, Zhou Z, Tang J, Liu X, Shen Y. *Adv Funct Mater*, 2017, 27: 1606826
102 Zhang Z, Wang Q, Liu Q, Zheng Y, Zheng C, Yi K, Zhao Y, Gu Y, Wang Y, Wang C, Zhao X, Shi L, Kang C, Liu Y. *Adv Mater*, 2019, 31: 1905751
103 Zhou L, Ding H, Zhao W, Hu S. *Spectrochim Acta Part A*, 2019, 206: 529–534
104 Sun X, Odyniec ML, Sedgwick AC, Lacina K, Xu S, Qiang T, Bull SD, Marken F, James TD. *Org Chem Front*, 2017, 4: 1058–1062
105 Van de Bittner GC, Dubikovskaya EA, Bertozzi CR, Chang CJ. *Proc Natl Acad Sci USA*, 2010, 107: 21316–21321
106 Viger ML, Collet G, Lux J, Nguyen Huu VA, Guma M, Foucault-Collet A, Olejniczak J, Joshi-Barr S, Firestein GS, Almutairi A. *Biomaterials*, 2017, 133: 119–131
107 Zhang G, Liao Q, Liu Y, Wang L, Gou H, Ke C, Huang X, Xi K, Jia X. *Nanoscale*, 2018, 10: 5503–5514
108 Mo R, Jiang T, Sun W, Gu Z. *Biomaterials*, 2015, 50: 67–74

109 Mo R, Jiang T, Gu Z. *Angew Chem Int Ed*, 2014, 53: 5815–5820
110 Qian C, Chen Y, Zhu S, Yu J, Zhang L, Feng P, Tang X, Hu Q, Sun W, Lu Y, Xiao X, Shen QD, Gu Z. *Theranostics*, 2016, 6: 1053–1064
111 Jiang C, Qi Z, Jia H, Huang Y, Wang Y, Zhang W, Wu Z, Yang H, Liu J. *Biomacromolecules*, 2019, 20: 478–489
112 Yoshinaga N, Ishii T, Naito M, Endo T, Uchida S, Cabral H, Osada K, Kataoka K. *J Am Chem Soc*, 2017, 139: 18567–18575
113 Zhou Z, Zhang Q, Zhang M, Li H, Chen G, Qian C, Oupicky D, Sun M. *Theranostics*, 2018, 8: 4604–4619
114 Zhou Z, Zhang M, Liu Y, Li C, Zhang Q, Oupicky D, Sun M. *Biomacromolecules*, 2018, 19: 3776–3787
115 Xu Z, Zeng G, Liu Y, Zhang X, Cheng J, Zhang J, Ma Z, Miao M, Zhang D, Wei Y. *Dyes Pigments*, 2019, 163: 559–563
116 Minami T, Emami F, Nishiyabu R, Kubo Y, Anzenbacher P. *Chem Commun*, 2016, 52: 7838–7841
117 Wang L, Yuan L, Zeng X, Peng J, Ni Y, Er JC, Xu W, Agrawalla BK, Su D, Kim B, Chang YT. *Angew Chem Int Ed*, 2016, 55: 1773–1776
118 Li J, Zhang N, Sun Q, Bai Z, Zheng J. *Talanta*, 2016, 159: 379–386
119 Gabrielli L, Carril M, Padro D, Mancin F. *Chem Eur J*, 2018, 24: 13036–13042
120 Qian CG, Zhu S, Feng PJ, Chen YL, Yu JC, Tang X, Liu Y, Shen QD. *ACS Appl Mater Interfaces*, 2015, 7: 18581–18589
121 Feng P, Chen Y, Zhang L, Qian CG, Xiao X, Han X, Shen QD. *ACS Appl Mater Interfaces*, 2018, 10: 4359–4368
122 Guo X, Wei X, Chen Z, Zhang X, Yang G, Zhou S. *Prog Mater Sci*, 2020, 107: 100599
123 Zhou Z, Shen Y, Tang J, Fan M, Van Kirk EA, Murdoch WJ, Radosz M. *Adv Funct Mater*, 2009, 19: 3580–3589
124 Pan L, He Q, Liu J, Chen Y, Ma M, Zhang L, Shi J. *J Am Chem Soc*, 2012, 134: 5722–5725
125 Pan L, Liu J, He Q, Shi J. *Adv Mater*, 2014, 26: 6742–6748
126 Zhu YX, Jia HR, Pan GY, Ulrich NW, Chen Z, Wu FG. *J Am Chem Soc*, 2018, 140: 4062–4070
127 Pan L, Liu J, Shi J. *Adv Funct Mater*, 2014, 24: 7318–7327
128 Tang R, Wang M, Ray M, Jiang Y, Jiang Z, Xu Q, Rotello VM. *J Am Chem Soc*, 2017, 139: 8547–8551
129 Wu R, Liu J, Chen D, Pan J. *ACS Appl Nano Mater*, 2019, 2: 4333–4341